RESEARCH ARTICLE
SPACE PHYSICS: MAGNETOSPHERIC PHYSICS

Earth and Planetary Physics
8: 299–306, 2024
doi: 10.26464/epp2023061

Analysis of the joint detection capability of the SMILE satellite and EISCAT-3D radar

JiaoJiao Zhang[1,2,3*], TianRan Sun[1,2,3], XiZheng Yu[3,4], DaLin Li[3,4], Hang Li[1,2,3], JiaQi Guo[3,4], ZongHua Ding[5], Tao Chen[1,2,3], Jian Wu[5], and Chi Wang[1,2,3]

[1]State Key Laboratory of Space Weather, National Space Science Center, Chinese Academy of Sciences, Beijing 100190, China;

[2]Key Laboratory of Solar Activity and Space Weather, National Space Science Center, Chinese Academy of Sciences, Beijing 100190, China;

[3]University of Chinese Academy of Sciences, Beijing 101408, China;

[4]Key Laboratory of Electronics and Information Technology for Space Systems, Chinese Academy of Sciences, Beijing 100190, China;

[5]China Research Institute of Radio-wave Propagation, Qingdao 266075, China

Key Points:

- An analysis of the joint detection capability of the SMILE satellite and EISCAT-3D radar was performed.
- A Web-based software program to search for and visualize the joint detection period of the SMILE satellite and EISCAT-3D radar was developed.
- The key scientific problems that can be solved by joint detection are summarized.

Citation: Zhang, J. J., Sun, T. R., Yu, X. Z., Li, D. L., Li, H., Guo, J. Q., Ding, Z. H., Chen, T., Wu, J., and Wang, C. (2024). Analysis of the joint detection capability of the SMILE satellite and EISCAT-3D radar. *Earth Planet. Phys.*, *8*(1), 299–306. http://doi.org/10.26464/epp2023061

Abstract: The Solar wind Magnetosphere Ionosphere Link Explorer (SMILE) satellite is a small magnetosphere–ionosphere link explorer developed cooperatively between China and Europe. It pioneers the use of X-ray imaging technology to perform large-scale imaging of the Earth's magnetosheath and polar cusp regions. It uses a high-precision ultraviolet imager to image the overall configuration of the aurora and monitor changes in the source of solar wind in real time, using in situ detection instruments to improve human understanding of the relationship between solar activity and changes in the Earth's magnetic field. The SMILE satellite is scheduled to launch in 2025. The European Incoherent Scatter Sciences Association (EISCAT)-3D radar is a new generation of European incoherent scatter radar constructed by EISCAT and is the most advanced ground-based ionospheric experimental device in the high-latitude polar region. It has multibeam and multidirectional quasi-real-time three-dimensional (3D) imaging capabilities, continuous monitoring and operation capabilities, and multiple-baseline interferometry capabilities. Joint detection by the SMILE satellite and the EISCAT-3D radar is of great significance for revealing the coupling process of the solar wind–magnetosphere–ionosphere. Therefore, we performed an analysis of the joint detection capability of the SMILE satellite and EISCAT-3D, analyzed the period during which the two can perform joint detection, and defined the key scientific problems that can be solved by joint detection. In addition, we developed Web-based software to search for and visualize the joint detection period of the SMILE satellite and EISCAT-3D radar, which lays the foundation for subsequent joint detection experiments and scientific research.

Keywords: Solar wind Magnetosphere Ionosphere Link Explorer (SMILE) satellite; European Incoherent Scatter Sciences Association (EISCAT)-3D radar; joint detection

1. Introduction

As human beings have entered the space age, space physics has developed rapidly. The sun–earth coupling problem has always been an important issue in space physics research. The Solar wind Magnetosphere Ionosphere Link Explorer (SMILE) satellite was jointly proposed by Chinese and European scientists to improve human understanding of the relationship between solar activity and the Earth's magnetic field. The SMILE satellite will operate at a large inclination and with a large elliptical orbit. It innovatively uses X-ray imaging technology to perform large-scale imaging of the dayside of the magnetopause and polar cusp regions and uses a high-precision ultraviolet imager to view the Earth's overall aurora borealis. The SMILE satellite also monitors changes in the source of solar wind in real time by using in situ detection instruments, thus forming a self-contained observation system. Unlike previous space physical exploration satellites, which could provide only single-point detection data, the SMILE satellite focuses on a global image of the magnetosphere and uses telemetry to understand the various regions of the Earth's magnetosphere and multiscale coupling phenomena on a macroscopic scale. Combined with in situ solar wind observation and remote

Correspondence to: J. J. Zhang, jjzhang@swl.ac.cn
Received 08 JUN 2023; Accepted 31 AUG 2023.
First Published online 08 SEP 2023.

sensing of the magnetosphere, the SMILE mission will provide the first panoramic imaging probe of solar wind–magnetosphere interactions that affect the entire space weather chain. In 2014, the SMILE satellite program emerged from the Sino-European joint space mission jointly initiated and implemented by the Chinese Academy of Sciences (CAS) and the European Space Agency (ESA). At the end of 2015, China and the European Union passed the review of the project proposal and began project approval (Wang C et al., 2017). The work was then performed in an orderly manner. In January 2022, the SMILE satellite underwent an extension test of the payload magnetometer at the European Space Technology Centre (ESTEC); in April 2022, the satellite payload module was tested in Europe and shipped to Shanghai, China, waiting to be integrated with the satellite platform; in February 2023, the SMILE mission satellite team went to the ESTEC of the ESA to perform the initial satellite–rocket joint test and successfully completed the interface docking, satellite separation, and impact tests. The SMILE satellite is expected to launch in 2025.

Incoherent scatter radar uses the weak incoherent scatter signal generated by random thermal fluctuations of the plasma in the ionosphere excited by the incident electromagnetic waves to remotely measure the physical parameters of the upper ionosphere. The cross section of ionospheric electron incoherent scatter radar is very small, and the scattered signal is very weak; thus, the transmitter power, receiver sensitivity, and antenna gain of the incoherent scatter radar are very high. Through spectral analysis of the incoherent scatter signal, information such as the electron temperature, ion temperature, and electron and ion drift velocity in the ionosphere can be obtained, and parameters such as the ionospheric conductivity, electric field, thermospheric wind, and collision frequency can be obtained indirectly. Since 1961, approximately 14 incoherent scatter radar systems have been established worldwide (Ding ZH et al., 2014). The European Incoherent Scatter Sciences Association (EISCAT) proposed building an incoherent scatter radar facility in Europe in the 1970s. The facility includes multistatic systems in the ultrahigh frequency (UHF) range and monostatic systems in the very high frequency (VHF) range. The working frequency band of EISCAT radar is divided into two frequency bands, VHF (224 MHz) and UHF (928 MHz). The transmitter is in Tromsø, Norway. The antenna of the VHF system is a parabolic cylinder; the UHF system is a three-station radar, and the receivers are in Sweden, Norway, and Finland. Since its establishment, EISCAT radar has played an important role in research on ionospheric ion outflow, auroral particle precipitation, small-scale plasma physics, magnetic reconnection, substorms, ionosphere–neutral atmosphere coupling, and the mesosphere. However, traditional incoherent scatter radar systems use high-power and high-voltage devices, which are complex and bulky, inconvenient for operation and maintenance, inflexible in their working modes, lacking in beamforming, and not fully satisfactory in temporal and spatial resolution. Moreover, the EISCAT incoherent scatter radar has been in place for 30 years; thus, the equipment is outdated, the maintenance and operation costs are high, and the radio in the UHF band (such as mobile communication) has serious interference and has stopped detection (Ding ZH et al., 2014). In recent years, with the rapid development of electronic technology, a new incoherent scatter radar based on the phased array system has been developed. In 2009, with the support of the National Science Foundation of the United States, the Stanford Research Institute of the United States built an advanced new generation of phased array incoherent scatter radar, AMISR, which has the characteristics of modularization, transportability, and expansion (Valentic et al., 2013). With the support of the EU framework agreement, in 2004, EISCAT began the demonstration, design, and preparation of the EISCAT-3D radar. The EISCAT aims to build a distributed phased array incoherent scatter radar system (with one central station and four receiving stations) that enables comprehensive three-dimensional (3D) vector observations of the atmosphere and ionosphere over northern Europe. Using new radar technology, combined with the latest digital signal processing, EISCAT-3D radar will achieve multibeam, multi-directional quasi-real-time 3D imaging capabilities, with a spatial and temporal resolution 10 times higher than existing radar systems, and will provide long-term continuous observations. In December 2008, EISCAT-3D was officially included in the development plan of the European Strategy Forum on Research Infrastructures (ESFRI). Between October 2010 and September 2014, 4-year preparatory work was begun, and the system entered the formal construction stage in 2016. The original plan was that all construction work would be completed by the end of 2021, although currently, the progress of the project is somewhat delayed. Construction of the central station and a receiving station was initiated in the autumn of 2021, and some antenna units were shipped to the station in the spring of 2022.

Cooperation between ground-based and space-based solar-terrestrial instruments will provide crucial multiscale details for the solar-terrestrial physical study (Carter JA et al, 2024). The SMILE satellite performs large-scale macroscopic detection of the coupled solar wind–magnetosphere–ionosphere system from top to bottom, whereas the EISCAT-3D radar performs multidirectional quasi-real-time 3D fine imaging of the polar ionosphere from bottom to top. For the SMILE satellite and EISCAT-3D, the joint detection of radar is expected to make important breakthroughs in the multiscale coupling of the solar wind–magnetosphere–ionosphere–thermosphere. By analyzing the joint detection capabilities of the SMILE satellite and EISCAT-3D radar, this work defines key scientific issues and condenses scientific goals, which will lay the foundation for follow-up scientific experiments of joint detection of the SMILE satellite and EISCAT-3D radar, for the formulation of a joint detection plan, and for results to be obtained quickly.

2. Description of the SMILE Satellite

With the aim of understanding global scientific issues involving the interaction between the solar wind and the magnetosphere, the scientific goals of the SMILE satellite are to detect the large-scale structure and basic patterns of the solar wind–magnetosphere interaction, to understand the overall change process and activity cycle of Earth's substorms, and to explore the occurrence

and development of coronal mass ejection-driven magnetic storms, thereby further understanding the impact of solar activities on the Earth's plasma environment and space weather.

The SMILE satellite is equipped with the following four payloads: a Soft X-ray Imager (SXI), an Ultraviolet Imager (UVI), a Light Ion Analyzer (LIA), and a digital magnetometer (MAG). The SXI obtains X-ray images of the magnetopause and polar cusp region on the dayside, the UVI images the distribution of the aurora borealis, the SXI and UVI cooperate with each other to realize panoramic imaging of the solar wind–magnetosphere interaction, and the LIA and MAG image the upstream solar wind driving source and perform in situ measurements.

The SMILE satellite operates in a large elliptical orbit with an apogee of 19 R_E (Earth radius), a perigee of 5000 km, and an argument of perigee of 280°. The precise inclination of the orbit is determined by the type of launch vehicle that launches the satellite. For example, the orbital inclination is 98.2° using the Soyuz rocket and the orbital inclination is 63°–100° using the Vega-C rocket (Wang C et al., 2017).

According to the type of payload, four types of scientific data are collected by the SMILE satellite:

(1) SXI data: Soft X-ray images with diffusive background, point sources, and particle background eliminated, and with the Vignetting function and Point spread function (PSF) considered.
(2) UVI data: Radiant intensity (in Rayleigh), the location of each pixel (latitude and longitude), and the location of the International Geomagnetic Reference Field magnetic footprint.
(3) MAG data: Total magnetic field B_t and magnetic field components B_x, B_y, and B_z.
(4) LIA data: Ion distribution function.

The SMILE SXI images the Earth's magnetosphere based on the principle of solar wind charge exchange. Sun TR et al. (2019) provided X-ray imaging results of the interaction between the solar wind and the magnetosphere by using a global magnetohydrodynamic (MHD) numerical simulation. Figure 1 shows the simulation results of the soft X-ray intensity based on the piecewise parabolic method with a Lagrangian remap to MHD (PPMLR–MHD) model during three different solar wind conditions, with the hypothetical satellite at [4.17, −9.70, 16.64] R_E and an SXI pointing to [8.72, 0, 0] R_E. The left panel (a) shows the X-ray images when the solar wind number density is 5 cm^{-3}, the solar wind velocity is 400 km/s, and the interplanetary magnetic field (IMF) B_z is −5 nT. Panels (b) and (c) show the X-ray images when the solar wind number density increases to 20 cm^{-3} and 35 cm^{-3}, respectively. The white lines in panel (a) mark the boundary positions for the northern and southern cusps, and the red lines show the mapping of the equatorial and noon–midnight meridian magnetopause. The crescent-shaped region with a relatively high intensity of X-ray radiation provides information on the location of the magnetopause boundary and is important for the study of system-level magnetospheric dynamics (Wang C and Branduardi-Raymont, 2020).

The UVI will be turned on in the satellite orbit above an altitude of 32,000 km to capture the aurora borealis. Because the SMILE satellite operates in a large elliptical orbit, the UVI will be able to observe the overall aurora borealis most of the time. A schematic diagram of the aurora observed by the UVI near the apogee of the satellite is shown in Figure 2. The red disc is the field of view of the UVI.

3. EISCAT-3D Incoherent Scatter Radar

The EISCAT-3D radar system consists of a central station with transmitting and receiving functions and four remote receiving stations. The stations are in Finland, Norway, and Sweden. The central site will be equipped with an antenna array of up to 10,000 individual antenna assemblies. The locations and coordinates of the alternative stations are shown in Table 1. Construction of the central station at Skibotn, Norway, and a receiving station at Karesuvanto, Finland, has already begun; the location of the other alternative stations may change depending on the specific situation.

The radar transmitter parameters are as follows:
• A center frequency of 233 MHz;
• A peak power output of 1000 W/antenna component, approximately 10 MW in total;
• An instantaneous 3 dB power bandwidth greater than 5 MHz;
• A pulse length of 0.5 to 3000 μs;
• A duty cycle of 0% to 25%;
• A pulse repetition period greater than 100 μs, and a fully flexible pulse sequence;
• Emissions with an arbitrary phase and amplitude;
• Stable gain and delay over the specified temperature range.

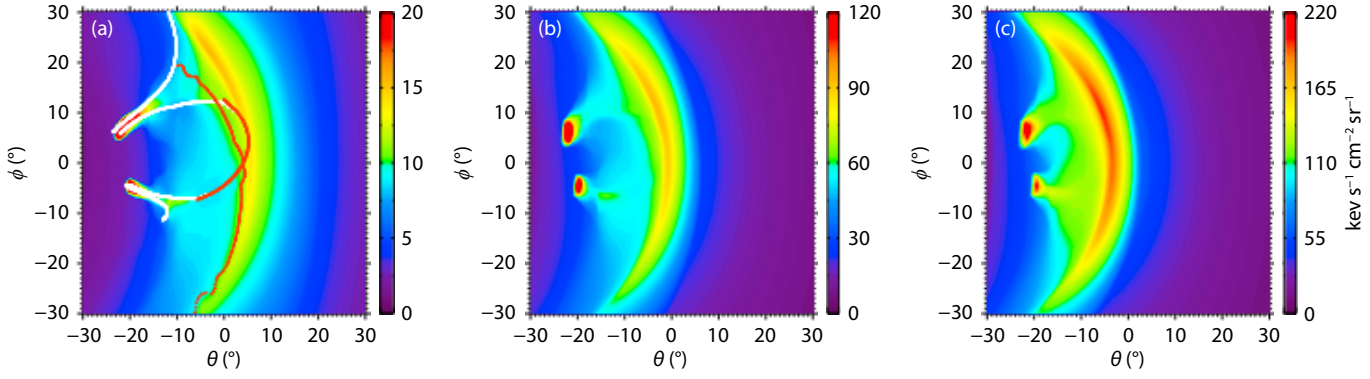

Figure 1. X-ray intensity at the magnetopause from an MHD numerical simulation. Adapted from Fig. 11 of Sun TR et al. (2019).

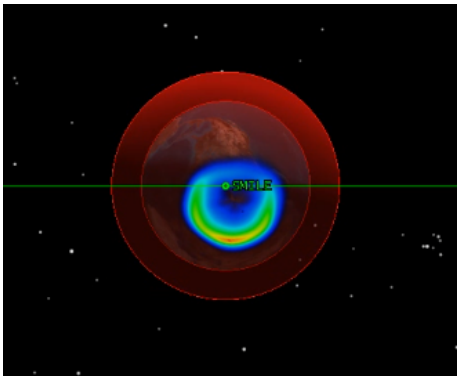

Figure 2. Schematic diagram of an aurora borealis image observed by the UVI on the SMILE satellite near the apogee of the satellite. The red disc is the field of view of the UVI.

Table 1. EISCAT-3D radar system candidate station coordinates.

Station	Country	Geographic latitude	Geographic longitude
Skibotn	Norway	69°21′N	20°20′E
Bergfors	Sweden	68°10′N	19°48′E
Karesuvanto	Finland	68°30′N	22°28′E
Andøya	Norway	69°8′N	15°52′E
Jokkmokk	Sweden	67°4′N	19°35′E

The receiver parameters are as follows:

• A center frequency of 233 MHz, or centered on the transmitting frequency;

• An instantaneous bandwidth of the main station ±15 MHz; other stations preferably a minimum of ±5 MHz;

• All additional noise temperatures (higher than sky noise) of less than 50 K;

• A spurious free dynamic range greater than 70 dB.

When the five stations of the EISCAT-3D radar system are completed, the detection capabilities of the EISCAT-3D radar at different altitudes (90, 110, and 300 km) for isotropic parameters and speeds will be the same as those shown in Figure 21 of a technical description document about EISCAT-3D (EISCAT Scientific Association, 2014). Data whose integration time is less than 0.1 s for scalar parameters and less than 1 s for vector parameters are high-quality data.

The EISCAT-3D has the ability to conduct multibeam and multidirectional quasi-real-time 3D imaging, obtain full-profile vector detection of ionospheric parameters, and take high-speed target tracking measurements. The EISCAT-3D is located in the auroral region, where complex and rich space weather phenomena occur. Through joint detection with incoherent scatter radar, the Super Dual Auroral Radar Network (SuperDARN), and satellites, the EISCAT-3D will have an important role in contributing to a deep understanding of the major scientific issues around the kinetic–chemical coupling process in the lower thermosphere; magnetosphere–ionosphere–thermosphere coupling; the coupling of the ionosphere at high, middle, and low latitudes; and the propagation characteristics of ionospheric disturbances.

4. Simulation Analysis of the Joint Detection Capability of the SMILE Satellite and EISCAT-3D Radar

4.1 Simulation Method

4.1.1 Satellite orbit

The SMILE satellite will operate in an inclined large elliptical orbit with an apogee altitude of 19 R_E and a perigee altitude of 5000 km. The specific orbital inclination will be determined by the type of launch vehicle. In this study, a satellite orbit with an inclination angle of 73° designed by the National Space Science Center of the Chinese Academy of Sciences was used for simulation. The ascending node right ascension for this orbit is 206°, the argument of perigee is 287.5°, and the true anomaly is 0°.

4.1.2 Parameter setting

To meet the scientific goals, in the satellite design, the attitude of the UVI points in the direction of the *Z* axis to the geocenter, the *Y* axis points from the sun to the satellite, and the *X* axis satisfies the right-hand screw rule. Its field of view is a cone field of view, with a half-beam angle of approximately 5° and a geocentric distance of 32,000 km or more for open-air observation, to perform large-scale and long-term observations of the aurora borealis. The orientation of the SXI is rotated 26° counterclockwise around the *X*-axis on the UVI coordinate system. Its field of view is a rectangular field of view of 16° × 27°, and the geocentric distance is greater than 50,000 km to perform imaging observations of the Earth's magnetosphere. For the SXI to calculate the observation period of the magnetopause and the polar cusps, we set three points in space to represent the typical positions of the magnetopause and the north and south polar cusps, as shown in Table 2. In the simulation, the valid detection altitude of the EISCAT-3D was set to 500 km, and the detection radius at this altitude was also set to 500 km. Figure 3 shows the SMILE satellite orbit, the SXI and UVI fields of view, the typical positions of the magnetopause, the north and south polar cusps, and the location and detection range of the EISCAT-3D radar.

4.1.3 Simulation method

We simulated the joint detection performance of the SMILE satellite and EISCAT-3D radar by comprehensively analyzing the satellite orbit; observation field; direction of the SXI, UVI, and EISCAT-3D radar positions; and observation field of view. Determination of the joint observation period of the UVI and EISCAT-3D was based on whether the field of view of the UVI intersected the observation range of the EISCAT-3D. In the calculation process, we calculated the field of view of the UVI at each moment and determined the intersection of the observation range of the EISCAT-3D and the field of view of the UVI. Determination of the joint observation period of the SXI and EISCAT-3D was based on the magnetic field lines, starting from the observation range of the EISCAT-3D and passing through the spatial range of the SXI field of view. In the calculation process, we calculated the magnetic field lines from the EISCAT-3D observation range and the SXI field of view at each moment and then determined whether the magnetic field lines intersected the SXI field of view.

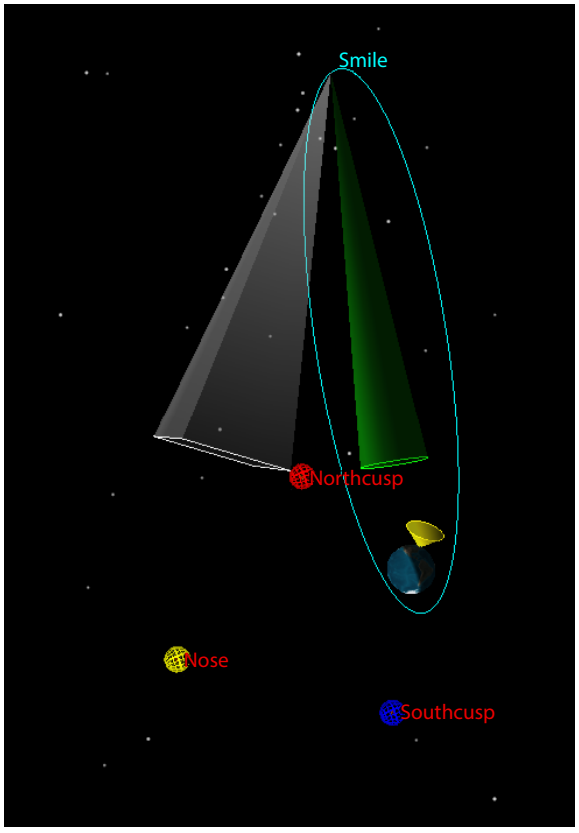

Figure 3. The SMILE satellite orbit, fields of view of the SXI and UVI, and locations of the magnetopause, north and south cusps, and EISCAT-3D radar.

Table 2. Locations of the magnetopause and the north and south polar cusps.

Name	Spatial location (GSM, R_E)
Magnetopause	[10, 0, 0]
North cusp	[2.8, 0, 5]
South cusp	[2.8, 0, −5]

4.2 Simulation Results

We now turn our attention to the simulation results. Figure 4 shows the simulation results of the jointly detectable period of the SMILE satellite UVI and EISCAT-3D radar in 2025. The abscissa is time and the ordinate is the orbital phase. As mentioned, the UVI will shut down when the geocentric distance is less than 32,000 km. The dark blue borders in Figure 4 indicate the shutdown times of the UVI. We can see that the shutdown time of the UVI is 18.42% of the total running time of the satellite. The rest of the time, the UVI has valid observations, which are 81.58% of the total running time and are indicated by purple in the figure. Note that most of the purple areas overlap the joint observation times of the UVI and EISCAT-3D radar, as indicated by the dusty blue color in Figure 4. We can see that the UVI and EISCAT-3D radar have a large joint detection time: 79.72% of the total running time is joint observation time. This is because the UVI in the design of the SMILE satellite mainly observes the aurora borealis, whereas the EISCAT-3D radar located in the polar region of the Northern Hemisphere is a powerful detection instrument for the observation of physical phenomena in the polar region; thus, the two have a high field of view overlap area.

The joint observation period of the SMILE satellite's SXI and UVI and the EISCAT-3D radar in 2025 is shown in Figure 5. The abscissa in the figure is the time and the ordinate is the orbital phase. Within these data, the SXI instrument's shutdown time, the no-target period when the instrument is turned on, the sun entering the field of view, and the Earth entering the field of view are periods when the instrument has no data. The SXI observation periods for the magnetopause and the north and south polar cusps are marked in different colors in the figure. We can see that the SXI instrument observes the magnetopause region (green) for most of the year and that a small portion of each orbital period from mid-February to early May observes the south polar cusp region (red). The north polar cusp (yellow) can be observed for a short period at relatively low orbital altitudes during each orbital period from January to August. The dark purple borders indicate the joint observation period of the SXI, UVI, and EISCAT-3D. There is a short period of time in each orbital period to realize the joint detection of SXI, UVI, and EISCAT-3D radar, and the joint detection period of

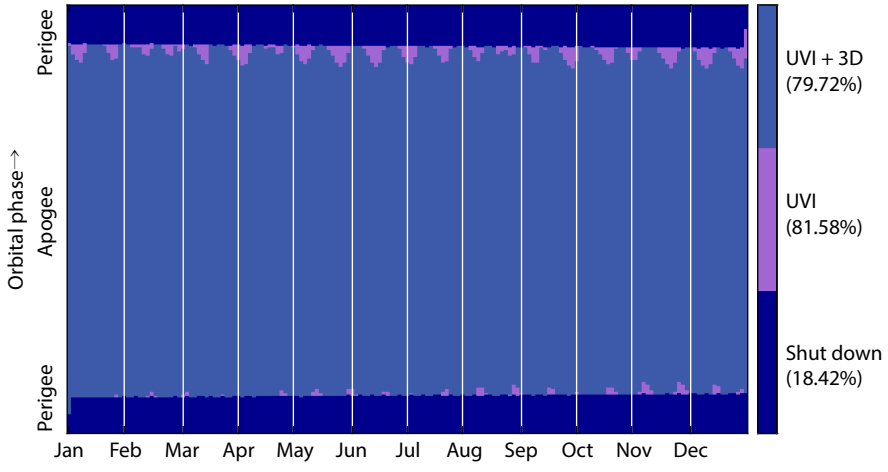

Figure 4. Joint detection period of the SMILE satellite's UVI and the EISCAT-3D during 2025.

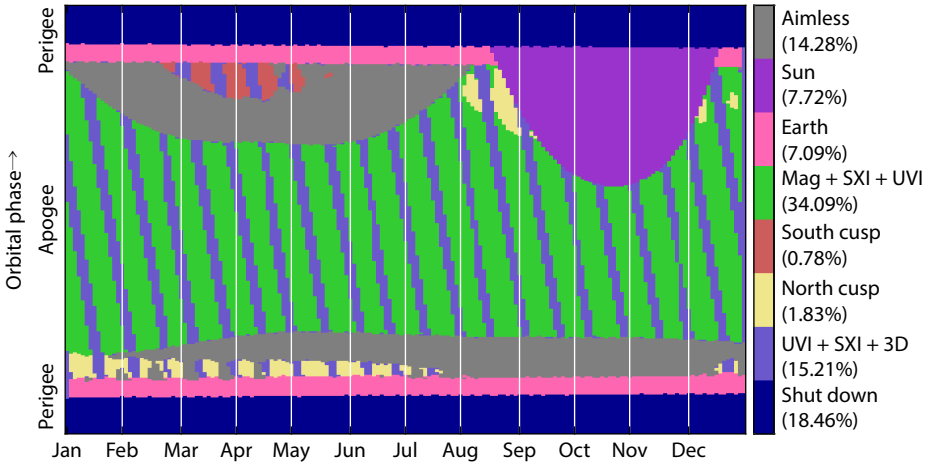

Figure 5. Joint detection period of the SMILE satellite's SXI and UVI and the EISCAT-3D during 2025.

the three instruments is 15.21% of the total satellite running time.

We now turn our attention to the jointly detectable period of the SXI, UVI, and EISCAT-3D during one orbit circle. Figure 6 shows the average jointly detectable period of the three instruments during one orbit circle for each month of the year of 2025. We can see from the figure that the jointly detectable period changes over the months. The longest jointly detectable period during one orbit circle is about 10 hours in January, and the shortest period is 5 hours in November. There are six months in which the average jointly detectable period during one orbit is more than 8 hours; they are January, February, March, April, May, and December.

It should be noted that determination of the joint observation period of the SXI and EISCAT-3D is based on the magnetic field lines starting from the observation range of the EISCAT-3D and passing through the spatial range of the SXI field of view. This is a very strict definition for joint observation. During this period, the variation in the magnetopause and cusp region observed by the SXI can be projected onto the ionosphere within the field of view of EISCAT-3D radar along the magnetic field line. On the other side, the EISCAT-3D radar should have several different observing modes during operation, but the radar is currently in the construction stage and no literature has been published on the observing mode, so this was not taken into account in the simulation. Nevertheless, the simulation results in this study will still serve as a reference and provide guidance on the design of radar observing modes to achieve certain scientific goals in a future joint detection plan. Furthermore, we will develop simulation models for specific scientific goals and radar observing modes based on the simulation in this study.

5. Simulation Software of the SMILE Satellite and EISCAT-3D Joint Detection

To facilitate scientific research users' search for the joint detection period, we developed joint detection simulation software for the SMILE satellite and EISCAT-3D radar based on Web technology. In 2027, data including the satellite position, equipment field of view, and effective detection period within a 3-year period will be visually displayed, and users will be provided with a joint detection period search function. The software interface is shown in Figure 7. The upper part displays the satellite position and the field of view of each instrument, the magnetic field lines from the EISCAT-3D radar, and the satellite and radar coordinates. The lower section shows a map of the combined instrument detection opportunities.

The main functions of the software include the following:

(1) The respective observation periods of the SXI, UVI, and EISCAT-

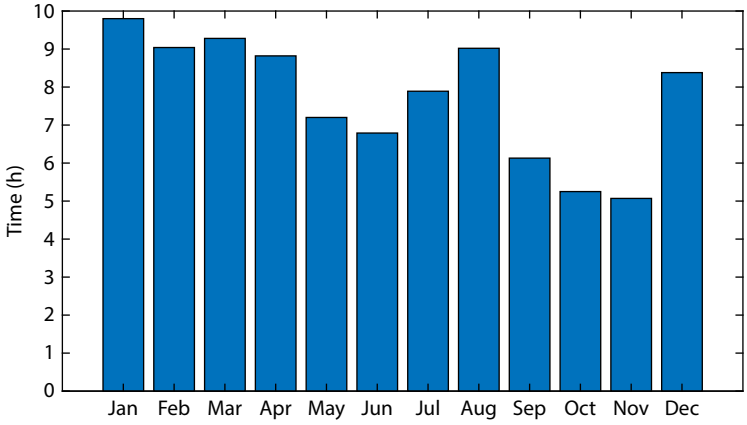

Figure 6. The average jointly detectable period of the SXI, UVI, and EISCAT-3D during one orbit circle for each month in the year of 2025.

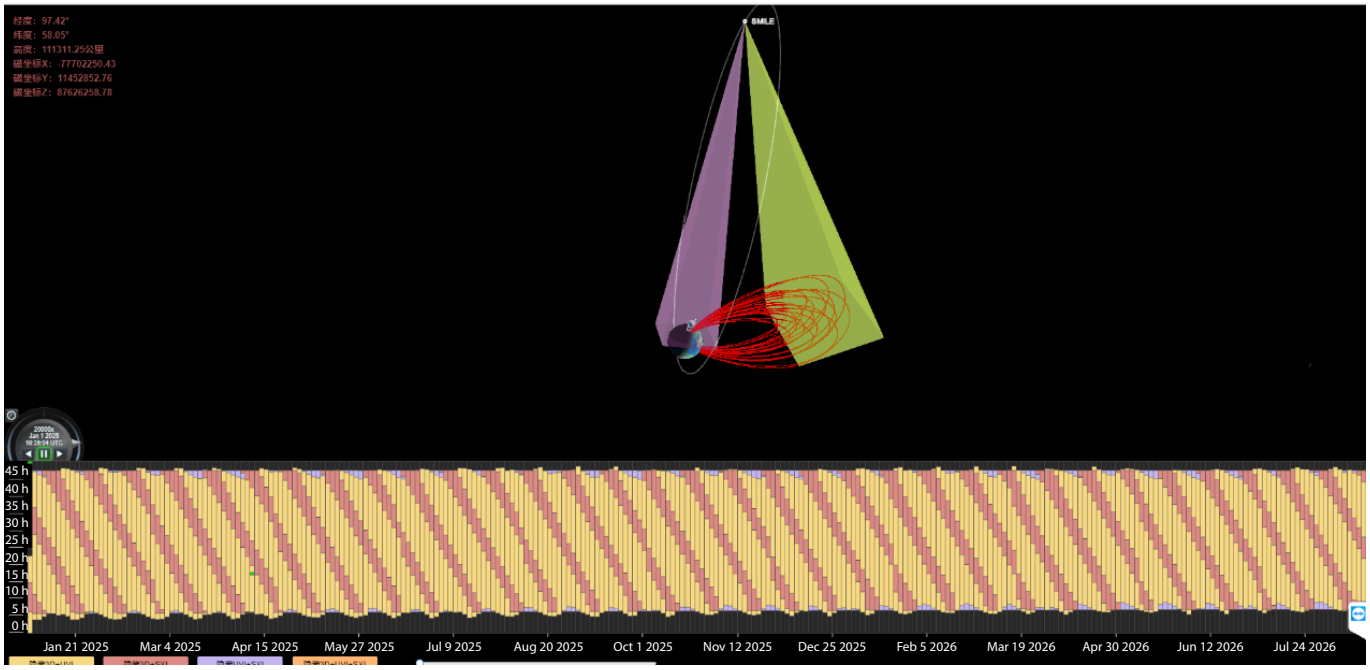

Figure 7. Human–computer interaction interface of the SMILE satellite and the EISCAT-3D radar joint detection simulation software.

3D radar; the SXI and UVI; the SXI and EISCAT-3D radar; the UVI and EISCAT-3D radar; and the SXI, UVI, and EISCAT-3D radar joint detection opportunities are displayed. Different colors are used for each type of joint detection opportunity, which is displayed on the subsection map of the instrument joint detection opportunity. The display and hiding of each type of detection opportunity can be independently controlled.

(2) Display of the SXI, UVI, and EISCAT-3D radar location and field of view at the selected time.

(3) Display of the satellite position at the selected time on the instrument joint detection opportunity division map.

(4) Display of the orbit range of the instruments' joint detection opportunity distribution diagram, which can be adjusted by setting the start and end times.

6. Determining Scientific Issues

The SMILE satellite will provide continuous global imaging of key regions of the solar wind–magnetosphere interaction on the dayside. The solar wind–magnetosphere interaction drives the magnetosphere into various response modes. Among various basic magnetospheric models, magnetic storms and substorms are the most common, are closely related to space weather, and are the basic models with which the scientific objectives of the SMILE satellite are most concerned. The satellite is expected to operate in orbit between 2025 and 2027, and it is expected to accumulate effective observation data for dozens of strong magnetic storms and 5000 substorms.

By measuring the size, shape, and curvature of the magnetopause as well as the location, width, and shape of the polar cusp regions, the SMILE satellite can resolve the different effects of dynamic pressure and magnetic reconnection in the global magnetospheric system. Furthermore, the nature, interaction mode, and main driving mechanism of solar wind–magnetosphere coupling can be resolved on a global scale. Satellite soft X-ray imaging will yield the location and shape of the magnetopause and polar cusp regions. The production of auroras reflects the activities of magnetic storms and substorms in the ionosphere. The SMILE satellite will continuously monitor the global shape and nature of the Earth's northern aurora and obtain many aurora observation images, thereby promoting the development of magnetospheric research.

The EISCAT-3D radar is in the auroral region, where complex and rich space weather phenomena occur. The joint detection by EISCAT-3D and the SMILE satellite can provide an in-depth understanding of major scientific issues in solar wind–magnetosphere–ionosphere–thermosphere coupling.

Through analysis, we can conclude that the aurora UVI of the SMILE satellite and the EISCAT-3D radar have a large amount of common observation time; the joint detection time accounts for 79.72% of the total running time of the satellite. Using the aurora borealis image data obtained by the satellite's UVI, the magnetospheric plasma data obtained by the low-energy plasma detector, the magnetic field strength obtained by the magnetometer, and the ionospheric–thermospheric temperature, density, composition, wind field, electric field changes, and other data obtained by the EISCAT-3D radar, the following research can be performed:

(1) Variation characteristics of auroras in the substorm activity cycle and the accompanying ionosphere–thermosphere coupling process.

(2) Characterization of the fine structure during large-scale changes of the aurora and the corresponding ionosphere–thermosphere coupling process.

(3) Magnetic storms and substorms that cause energy dissipation and heating in the polar regions.

The SMILE satellite's SXI and aurora UVI and the EISCAT-3D radar

can jointly detect approximately 15% of the total satellite operating time. Using these time periods for joint detection is expected to lead to breakthroughs in the following scientific issues:

(1) The difference between the auroras corresponding to steady-state and transient magnetopause reconnection processes, and the similarities and differences in the ionosphere–thermosphere coupling process.
(2) Under different solar wind parameters (such as β value), IMF clock angles, and Mach numbers, the transport pathways and quantitative estimations of solar wind energy and matter in magnetospheric space, the ionosphere, and the thermosphere.
(3) The magnetospheric substorm period, including its time sequence and flux transmission intensity, and the ionospheric–thermospheric characteristics of each stage.
(4) How open magnetic flux controls the occurrence and development of substorms and ionospheric–thermospheric changes.
(5) Proton bright spots and associated reconnection-driven plasma transport processes in the cusp region.

7. Conclusions

The SMILE satellite is a small satellite for magnetosphere detection that was developed cooperatively between China and Europe. It uses X-ray imaging technology to perform large-scale imaging of the Earth's magnetopause and polar cusp areas and provides imaging detection of the overall configuration of the aurora through a high-precision UVI. In situ detection instruments are used to monitor changes in the source of solar wind in real time to improve human understanding of the relationship between solar activity and changes in the Earth's magnetic field. The EISCAT-3D radar is the most advanced ground-based ionospheric experimental device in the high-latitude polar regions, representing the latest development direction and level of ground-based detection radar for the current space environment. The main technical features of EISCAT-3D include multibeam, multidirectional, quasi-real-time 3D imaging capability, a multiple-station configuration with one transmitter and four receivers, continuous operation monitoring capability (limited only by the power supply and the disk data storage capacity), and multiple-baseline interferometry ability. Using the SMILE satellite and EISCAT-3D radar to detect the coupled process of magnetosphere–ionosphere dynamics is of great scientific significance.

On the basis of the planned orbit of the SMILE satellite, the observation field of view of each piece of equipment, and other parameters, we performed a joint detection analysis of the SMILE satellite and the EISCAT-3D radar and analyzed the joint detection capability of the two systems. The results showed that the SMILE satellite's UVI and the EISCAT-3D radar have a large amount of joint detection time; the joint observation time accounts for 79.72% of the total running time. The combined detection time of the SMILE satellite's SXI and UVI and the EISCAT-3D radar is 15.21% of the total running time. The simulation software gives the orbital phase of the joint detection and the time period during which the joint detection can be performed. We developed the Web-based SMILE satellite and EISCAT-3D joint detection human–computer interaction software, which provides a powerful means for selecting experimental windows for the subsequent joint detection.

We analyzed the following key scientific questions around magnetosphere–ionosphere–thermosphere coupling that can be solved by the combined detection of the SMILE satellite and EISCAT-3D radar: What are the auroras corresponding to the steady-state and transient magnetopause reconnection processes and their ionosphere? What are the similarities and differences in the thermal layer coupling process? What are the magnetospheric substorm cycles, including their timing process and flux transmission intensity and the ionospheric–thermospheric characteristics of each stage? How do open magnetic fluxes control the occurrence and development of substorms and ionospheric–thermospheric changes? What is the relationship between the ring current or partial ring current and the position of the magnetopause during a magnetic storm, as well as changes in the aurora, ionospheric density, temperature, and wind field during the development of a magnetic storm?

This research analyzes the joint detection capability of the SMILE satellite and EISCAT-3D radar, determines key scientific issues, condenses scientific goals, and has developed joint detection human–computer interaction software, which lays a good foundation for subsequent joint detection experiments and scientific research.

Acknowledgments

This work was supported by the Stable-Support Scientific Project of the China Research Institute of Radio-wave Propagation (Grant No. A13XXXXWXX), the National Natural Science Foundation of China (Grant Nos. 42174210, 4207202, and 42188101), and the Strategic Pioneer Program on Space Science, Chinese Academy of Sciences (Grant No. XDA15014800).

References

Carter, J. A., Dunlop, M., Forsyth, C., Oksavik, K., Donovon, E., Kavanagh, A., Milan, S. E., Sergienko, T., Fear, R. C., … Zhang, Q.-H. (2024). Ground-based and additional science support for SMILE. *Earth Planet. Phys.*, *8*(1), 275–298. https://doi.org/10.26464/epp2023055

Ding, Z. H., Dai, L. D., Dong, M. Y., Xu, Z. W., and Wu, J. (2014). Progress of the incoherent scattering radar: from the traditional radar to the latest EISCAT 3D. *Prog. Geophys.* (*in Chinese*), *29*(5), 2376–2381. https://doi.org/10.6038/pg20140557

EISCAT Scientific Association. (2014). *EISCAT_3D: The Next Generation International Atmosphere and Geospace Research Radar*. Techical Description.

Sun, T. R., Wang, C., Sembay, S. F., Lopez, R. E., Escoubet, C. P., Branduardi-Raymont, G., Zheng, J. H., Yu, X. Z., Guo, X. C., … Guo, Y. H. (2019). Soft X-ray imaging of the magnetosheath and cusps under different solar wind conditions: MHD simulations. *J. Geophys. Res.*: *Space Phys.*, *124*(19), 2435–2450. https://doi.org/10.1029/2018JA026093

Valentic, T., Buonocore, J., Cousins, M., Heinselman, C., Jorgensen, J., Kelly, J., Malone, M., Nicolls, M., and Van Eyken, A. (2013). AMISR the advanced modular incoherent scatter radar. In *Proceedings of 2013 IEEE International Symposium on Phased Array Systems and Technology* (pp. 659–663). Waltham, MA, USA: IEEE. https://doi.org/10.1109/ARRAY.2013.6731908

Wang, C., Li, Z. J., Sun, T. R., Liu, Z. Q., Liu, J., Wu, Q., Zheng, J. H., and Li, J. (2017). SMILE satellite mission survey. *Space Int.* (*in Chinese*), (8), 13–16. https://doi.org/10.3969/j.issn.1009-2366.2017.08.003

Wang, C., and Branduardi-Raymont, G. (2020). Update on the ESA-CAS joint Solar wind Magnetosphere Ionosphere Link Explorer (SMILE) mission. *Chin. J. Space Sci.*, *40*(5), 700–703. https://doi.org/10.11728/cjss2020.05.700